Available online at www.sciencedirect.com
SCIENCE DIRECT®
PERGAMON
Vision Research 43 (2003) 1983–2001
Vision Research
www.elsevier.com/locate/visres

Coding of the contrasts in natural images by populations of neurons in primary visual cortex (V1)

P.L. Clatworthy, M. Chirimuuta *, J.S. Lauritzen [1], D.J. Tolhurst

Department of Physiology, University of Cambridge, Downing Street, Cambridge CB2 3EG, UK

Received 23 November 2001; received in revised form 17 December 2002

Abstract

It is possible to discriminate between grating contrasts over a 300-fold contrast range, whereas V1 neurons have very limited dynamic ranges. Using populations of model neurons with contrast-response parameters taken from electrophysiological studies (cat and macaque), we investigated ways of combining responses to code contrast over the full range. One model implemented a pooling rule that retained information about individual response patterns. The second summed responses indiscriminately. We measured accuracy of contrast identification over a wide range of contrasts and found the first model to be more accurate; the mutual information between actual and estimated contrast was also greatest for this model. The accuracy peak for the population of cat neurons coincided with the peak of the distribution of contrasts in natural images, suggesting an ecological match. Macaque neurons seem better able to code contrasts that are slightly higher on average than those found in the natural environment.
© 2003 Elsevier Science Ltd. All rights reserved.

Keywords: Contrast; Natural images; Histogram equalisation; V1; Visual cortex; Striate cortex

1. Introduction

It is a popular tenet that visual systems are suited to the tasks they must carry out (e.g. Atick, 1992; Barlow, 1989; van Hateren, 1992; Laughlin, 1983; Lythgoe, 1991; Marr, 1982). One implication is that the mammalian visual system is suited to tasks involving natural images, or stimuli with statistics typical of natural images. This has been argued from studies of receptive-field organisation or spatial tuning of neurons (Atick & Redlich, 1992; Baddeley & Hancock, 1991; Burton & Moorhead, 1987; Dan, Atick, & Reid, 1996; Field, 1987; van Hateren & van der Schaaf, 1998; Law & Cooper, 1994; Scwartz & Simoncelli, 2001; Srinivasan, Laughlin, & Dubs, 1982), the spectral absorption of cones (Osorio & Vorobyev, 1996; Regan et al., 2001) or the psychophysics of complex-scene discrimination (Geisler, Perry, Super, & Gallogly, 2001; Knill, Field, & Kersten, 1990; Parraga, Troscianko, & Tolhurst, 2000; Tadmor & Tolhurst, 1994; Thomson & Foster, 1997; Tolhurst & Tadmor, 2000).

Natural images contain a wide range of contrasts, the distribution of which is not uniform (Brady & Field, 2000; Laughlin, 1981; Lauritzen & Tolhurst, 2000; Tadmor & Tolhurst, 2000; Tolhurst, 1996). Behavioural and psychophysical performance of animals and humans in contrast identification and discrimination tasks also vary with contrast in a non-uniform manner (Blake & Petrakis, 1984; Bradley & Ohzawa, 1986; Campbell & Kulikowski, 1966; Foley, 1994; Itti, Koch, & Braun, 2000; Kiper & Kiorpes, 1994; Legge & Foley, 1980; Nachmias & Sansbury, 1974; Tolhurst & Barfield, 1978). One might hypothesise that this variation in performance is matched to the differential distribution of contrasts to which the animal has been exposed. This matching could have occurred gradually over an evolutionary time-scale, whereby the ability to identify contrast well gives a selective advantage, or over an individual's lifetime (possibly during a brief critical period) as a result of a plastic visual system, or both.

* Corresponding author. Tel.: +44-1223-333884; fax: +44-1223-333840.
E-mail address: mc325@cam.ac.uk (M. Chirimuuta).
[1] Present address: Vision Science Research Group, School of Biomedical Sciences, University of Ulster, Coleraine BT52 1SA, Northern Ireland, UK.

0042-6989/03/$ - see front matter © 2003 Elsevier Science Ltd. All rights reserved.
doi:10.1016/S0042-6989(03)00277-3

Laughlin (1981) deduced a specific ecological match between a simple contrast measure in natural images and the responses of fly visual neurons. He measured contrast-response functions of neurons using spot stimuli of known Weber contrast. Contrasts in natural images were calculated from one-dimensional luminance scans of the images. The sigmoidal contrast-response functions of the neurons followed closely the cumulative probability distributions of contrasts in the natural images; the non-uniform input distribution of contrasts is mapped through a neuron's non-linear contrast-response function so that all possible discrete responses of the neuron are equally likely. Laughlin (1981) suggested that the match between the contrast-response function of a neuron and the cumulative distribution of natural contrasts is akin to "histogram equalisation": each fixed increment of response amplitude codes for a fixed proportion of contrast occurrences. The neuronal responses would be particularly efficient at encoding the contrasts in natural scenes because the code would have maximum entropy. Tadmor and Tolhurst (2000) performed analogous comparisons for cat and monkey retinal and lateral geniculate nucleus (LGN) neurons, using two-dimensional greyscale images, and they showed a similar relationship between cumulative distributions of image contrast and most neuronal responses. This relationship was not, however, evident for LGN cells in the monkey parvocellular pathway.

When we study the visual cortex, however, a simple histogram equalisation is unlikely to be appropriate, since the variance of cortical responses is multiplicative, changing with response level (Dean, 1981b; Geisler & Albrecht, 1997; Tolhurst, Movshon, & Thompson, 1981, 1983; Vogels, Spileers, & Orban, 1989; Wiener, Oram, Liu, & Richmond, 2001) whereas at lower levels in the visual system the variability is additive (Croner, Purpura, & Kaplan, 1993; Kremers, Silveira, & Kilavik, 2001). Rather than equal increments of response magnitude, it is more likely that each *equally discriminable* increment of response (e.g. d' steps) would code for a fixed proportion of contrast occurrences.

The contrast-response functions of single neurons in the retina and LGN may be suited to and are, perhaps, determined by the contrasts encountered in the natural environment. However, contrast-response functions of neurons in the visual cortex are quite different. They too are sigmoidal, but with dynamic ranges much narrower than the range of contrasts found in natural images (Albrecht & Hamilton, 1982; Dean, 1981a; Sclar, Maunsell, & Lennie, 1990; Tolhurst et al., 1981, 1983). The differential firing of a single neuron would therefore be unable to encode the whole variety of contrasts in the natural environment. If the full range of contrasts is to be encoded, there must be *pooling* of the responses of populations of neurons with dynamic ranges centred on different parts of the contrast range.

It is not certain how neuronal responses are pooled. One possible method might be simple summation of activity across the neurons in a population, with this summed activity being used to identify contrast (cf. Boynton, Demb, Glover, & Heeger, 1999; Britten, Shadlen, Newsome, & Movshon, 1992; Heeger, Huk, Geisler, & Albrecht, 2000). This method does not take account of any information available in the *differential activity* of each neuron. For example, if a neuron responsive only to high contrasts were to generate an action potential, that would be a sure sign that the contrast was high. However, if that single action potential were simply added in to a population response, it would be swamped by the larger, noisy responses of neurons that are responsive to low contrasts as well as to high. Geisler and Albrecht (1995, 1997) used signal detection theory to model the identification and discrimination of contrasts by single neurons. Performance of populations of neurons was calculated using Bayesian decision theory. Such a model *does* account for the differential activity of different neurons, as well as for any response-dependent variability.

In this paper, we describe two computational models of mammalian simple cells in a contrast identification task. We compare the performance of individual neurons and of two realistic populations of neurons, having response parameters taken from studies in cat and macaque monkey with the distribution of contrasts in natural images, calculated using an "equivalent contrast" metric (Brady & Field, 2000; Tadmor & Tolhurst, 2000). For populations of neurons, two neural pooling methods are compared. Both are based on a Bayesian maximum *a posteriori* estimate of contrast, but one takes account of the differential responses of all of the neurons whereas the other takes account only of the summed firing rates of the neurons. For both models, the neuron population modelled on neurophysiological data from cat is most accurate at identifying those contrasts which are most prevalent in natural images. However, for the population of neurons modelled on monkey data, the most accurately identified contrasts match natural image contrasts slightly less well. Some of this work has been reported briefly (Clatworthy, Chirimuuta, Lauritzen, & Tolhurst, 2001; Lauritzen & Tolhurst, 2000; Tolhurst, 1996).

2. Methods

2.1. Modelling cortical neuronal contrast-response functions

The mean response, μ, of a neuron to presentation of a grating of contrast, c, was modelled according to Eq. (1) (Naka & Rushton, 1966), which approximates to the contrast-response function of mammalian striate cortex

neurons (Albrecht & Hamilton, 1982; Gardner, Anzai, Ohzawa, & Freeman, 1999; Sclar et al., 1990; Tolhurst & Heeger, 1997),

$$\mu = R_{\max} \frac{c^q}{c_{50}^q + c^q} \quad (1)$$

where μ is the mean number of action potentials produced during one "presentation" of contrast, c, in a contrast identification task; $R_{\max}$ is the mean neuronal response at which full saturation is reached; c_{50} (the *semi-saturation contrast*) is the contrast at which the mean response equals half $R_{\max}$. The exponent, q, has an average value of about 2 for cortical neurons in cat and monkey (Albrecht & Hamilton, 1982; Sclar et al., 1990). In fact, Heeger (1992a, 1992b) models neuronal responses with the Naka–Rushton equation with an exponent of *exactly* 2, based on the hypothesis that striate cortical neurons are encoding contrast *energy*. Gottschalk (2002) also shows that an exponent of 2 is ideal for information transmission under certain constraints. In our study, therefore, q takes a value of 2 for almost all of our simulations. We have also examined a formulation in which the neurons are modelled as having a "hard threshold": two percent of $R_{\max}$ is subtracted from μ in Eq. (1), and, when the result is negative, it is set to zero.

A sinusoidal grating has Michelson contrast, c, defined as

$$c = \frac{L_{\max} - L_{\min}}{L_{\max} + L_{\min}} \quad (2)$$

where $L_{\max}$ and $L_{\min}$ are the maximum and minimum values of luminance in the grating.

The variance of distributions of neuronal responses to presentation of a contrast is, to a good approximation, proportional to the mean response (see also Kontsevich, Chen, & Tyler, 2002); the variance exceeds the mean by a factor of about 2 (Dean, 1981b, Geisler & Albrecht, 1997; Tolhurst et al., 1981, 1983; Vogels et al., 1989; Wiener et al., 2001). For our model, the probability density function (pdf) of a neuron's response to one "presentation" of a contrast (one "trial") was calculated by combining two sets of Poisson probability density function. Effectively we could build up the response pdf $P(r|c)$ by sampling many times from the Poisson distributions; the first Poisson, with parameter μ calculated from Eq. (1), gave an integer value, x, which was used as the parameter for a second Poisson decision. This second Poisson gave a value that was the neuron's final integer response, r, to that contrast on that trial. This method gave a pdf of neuronal responses, $P(r|c)$, similar to that of a Poisson distribution (see Fig. 1A), but with a variance twice its mean.

Thus, for a given mean response, μ, the first Poisson would give events of magnitude x with probability:

$$P(x) = \frac{e^{-\mu} \cdot \mu^x}{x!} \quad (3)$$

and the probability of a given action potential count, r, at a given contrast, c, after sampling from the second Poisson is given by

$$P(r|c) = \sum_x \left(P(x) \frac{e^{-x} \cdot x^r}{r!} \right) \quad (4)$$

Examples of modelled single neuron contrast-response functions are shown in Fig. 1A and B. Fig. 1A also shows sample response distributions based on different mean responses (labelled (i) to (iii)). It can be seen that the distributions of responses for individual neurons are not normally distributed, but become closer to being normal as the mean response increases, as is the case for a simple Poisson distribution (Tolhurst, 1989). The error bars in Fig. 1A and B are the square roots of the variance. They are drawn symmetrically about the mean, but clearly at low contrast the response distribution is not and cannot be symmetrical. It can be seen, however, that the standard deviation of the response distribution increases with the mean. Although the form of the contrast-response function is identical for $R_{\max}$ values of 10 (Fig. 1A) and 100 (Fig. 1B), the proportionate variation in response is very different. This has implications for how precisely contrast can be estimated, based on the responses of each neuron. It might be expected that increasing $R_{\max}$ (thereby decreasing the coefficient of variation) would increase the ability of the neuron to encode contrast accurately (cf. Tolhurst, 1989).

2.2. Estimation of contrast from neuronal responses using a Bayesian method

In order to model how individual neurons and populations of neurons perform in contrast identification tasks, we used a Bayesian maximum a posteriori method. For each neuron, we calculated the probability that each contrast in our model's range of contrasts might have been presented, $P(c|r)$, contingent on the neuron's response:

$$P(c|r) = \frac{P(r|c) \cdot P(c)}{P(r)} \quad (5)$$

$P(r|c)$ was given by the pdf of our neuronal response distribution, as calculated from Eqs. (3) and (4). $P(r|c)$ was calculated for 311 contrasts, covering the range of contrasts from 0.001 to 1.26 in logarithmic steps. Obviously, we cannot have a sinusoidal grating with contrast greater than 1.0; however, it is possible for a neuron with band-pass tuning to encounter stimuli whose *effective* contrast exceeds unity (e.g. the fundamental of a square wave grating of unit contrast).

$P(c)$ is the *prior probability* of a contrast being presented in a trial. In a natural setting this might be the relative frequency of that contrast in the environment (see below). In our model, however, a finite range of contrasts was used and, in most procedures, we presumed

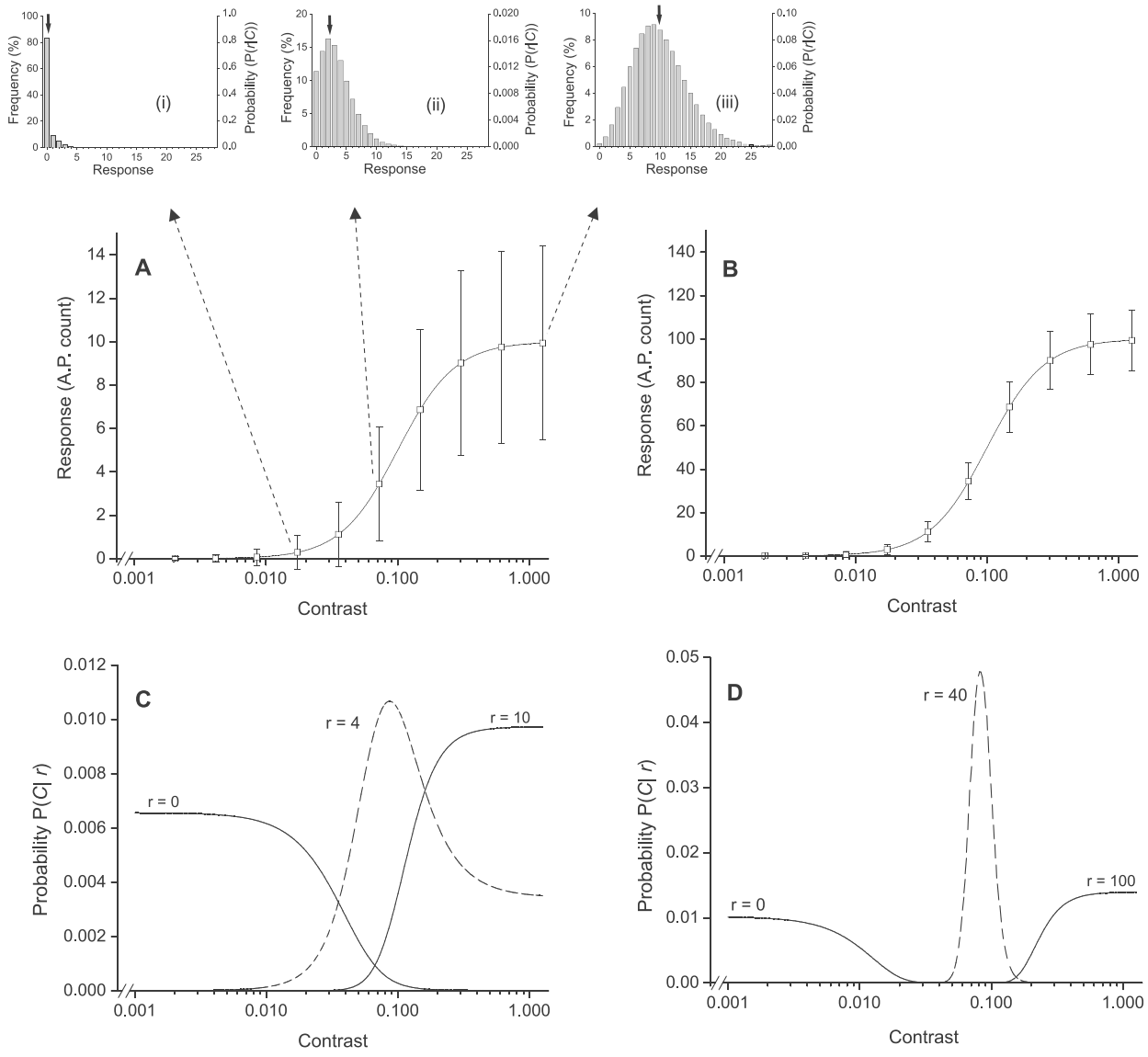

Fig. 1. Single neuron contrast-response functions and probability distributions $P(c|r)$. (A) Naka–Rushton contrast-response function for a model single neuron with R_{max} of 10, q of 2 and c_{50} of 0.1. Symbols with error bars are examples of mean responses, μ and the square roots of the response variance. Probability density function (pdf) of responses, $P(r|c)$, for this neuron and mean responses of (i) 0.29, (ii) 3.44 and (iii) 9.94 are shown. The arrows indicate the mean response values, μ. The shape of the distributions becomes closer to a normal distribution at high mean response rates. (B) Model single neuron contrast-response function for R_{max} of 100, q of 2 and c_{50} of 0.1. The error bars are much smaller proportionately than in (A), since the variance of the responses are still roughly twice the mean response and the error bars represent the square roots of the variances. (C) Posterior probability distributions, $P(c|r)$, for the neuron shown in (A) and responses, r, of 0, 4 and 10 action potentials. (D) $P(c|r)$ distributions for the neuron shown in (B), for responses of 0, 40 and 100. The curves are sharper than in (C), indicating less variation in the distributions.

that each contrast was equally likely to be present, i.e. $P(c)$ is uniformly distributed across the 311 contrasts. We did, however, examine the effect of accounting for the non-uniform distribution in natural images (Fig. 8).

$P(r)$ was determined according to:

$$P(r) = \sum_{c} P(r|c) \tag{6}$$

Fig. 1C and D show calculated posterior probability distributions based on different neuron response values, r, for two values of R_{max} (10 and 100). Consistent with the relatively small standard deviation of the responses of the model neuron with higher R_{max} (Fig. 1D), the functions relating $P(c|r)$ to contrast for this neuron are sharper than for the neuron with lower R_{max} (Fig. 1C).

2.3. Accuracy of contrast identification by a single neuron

For each of the 311 contrasts used, a mean neuronal response, μ was calculated using Eq. (1), and from this a pdf $P(r|c)$, was calculated according to Eqs. (3) and (4).

10,000 trials of a contrast identification task were simulated for each contrast. On every trial a single response, r, was sampled at random from vector $P(r|c)$, and vector $P(c|r)$ was calculated from this according to Eq. (5). For a single neuron, the estimate of contrast made by the model was that for which the posterior probability $P(c|r)$ was a maximum.

The performance measure used to evaluate the accuracy of the model's prediction of presented contrast was the inverse of the squared difference between the logarithms of estimated ($\hat{c}$) and actually presented (c) contrasts, averaged over the 10,000 (t) trials. This measure of accuracy is similar to the inverse of the variance of the contrast estimates, but whereas a large persistent systematic error might give a small variance, our performance measure would give an appropriately poor accuracy:

$$\text{accuracy} = \frac{t}{\sum_t \Big(\log(\hat{c}) - \log(c)\Big)^2} \tag{7}$$

2.4. Populations of neurons

When the contrast identification accuracy of a population of n neurons was modelled, two methods of neural pooling were compared:

For the first pooling method (cf. Geisler & Albrecht, 1997), the overall posterior probability $P(c|\mathbf{r})$ for a population of n neurons was calculated by combining the individual posterior probabilities according to Eq. (8), where $\mathbf{r}$ is the set of n individual responses $[r_1, r_2, r_3, \ldots, r_n]$, and $P(c|r_i)$ is the probability of a given contrast given that the ith neuron gave a response r_i

$$P(c|\mathbf{r}) = \frac{\prod_n P(c|r_i)}{P(\mathbf{r})} = \frac{\prod_n P(c|r_i)}{\prod_n P(r_i)} \tag{8}$$

For the second pooling method (cf. Boynton et al., 1999; Britten et al., 1992; Heeger et al., 2000), the outputs of the n neurons were simply summed, to give a combined response, R, which was then used to estimate contrast in the same manner as for single neurons, as described by (compare Eq. (5)):

$$R = \sum_{i=1}^{n} r_i \tag{9}$$

$$P(c|R) = \frac{P(R|c) \cdot P(c)}{P(R)} \tag{10}$$

$P(R)$ and $P(R|c)$ were not be calculated explicitly, but were built up by many simulations of the responses, r_i, of the n neurons.

2.5. Calculating the contrasts in natural images

Contrasts were calculated for a set of 64 grey-scale images of a variety of natural scenes (Tolhurst, Tadmor, & Chao, 1992). Monochrome photographs were digitised, giving grey-scale images of 256-by-256 pixels and with over 1000 grey levels. Calibration against Munsell grey-paper charts accounted for any non-linearities in the camera and film, so that pixel value was directly proportional to luminance. The images were not scaled to fit the available grey levels; the lowest pixel value represented the lowest luminance present in the scene. Image content was representative of the type of scene encountered by the visual system during its everyday experience, and included plants, animals, landscapes, buildings, people, faces and still life.

Contrasts in these natural images were calculated using the "equivalent contrast" method (Brady & Field, 2000; Tadmor & Tolhurst, 2000; Tolhurst, 1996). Odd-symmetric Gabor filters were used as local contrast operators, these having similar receptive-field properties to simple cells in striate cortex (Field & Tolhurst, 1986; Jones & Palmer, 1987; Marcelja, 1980). We did not use even-symmetric Gabor filters since these have a d.c. response and are not, therefore, ideal models of real simple cells (Field & Tolhurst, 1986). Eight spatial frequencies in logarithmic steps from 3 to 32 cycles per image, at 8 evenly spaced orientations were used in all possible combinations, giving 64 filters. We performed calculations with several sets of filters with spatial-frequency bandwidths ranging from 1.0 to 2.0 octaves (full width at half height). Orientation bandwidths for the filter sets were approximately 22°–48° (half width at half height). Bandwidth values for spatial frequency and orientation thus accorded well with data from cat and monkey striate cortex (De Valois, Albrecht, & Thorell, 1982; De Valois, Yund, & Heppler, 1982; Ikeda & Wright, 1975; Movshon, Thompson, & Tolhurst, 1978; Tolhurst & Thompson, 1981).

Each of the 64 natural images was convolved with each of the 64 Gabor filters. The images were also convolved with two-dimensional Gaussians with the same spreads as the Gabors, to provide an estimate of the mean luminance within each filter's "receptive field". The filter-response was divided by the appropriate Gaussian-response to model light adaptation, thereby giving a 256×256 image corresponding to the *contrast response* of the filter (cf. Peli, 1990). Some authors take the logarithms of the pixel values as their model of light adaptation and contrast coding, before performing subsequent linear stages (e.g. Brady & Field, 2000; van Hateren & van der Schaaf, 1998); there is no neurophysiological guidance as to which is a better model of contrast coding.

In order to relate these response values to contrast values, we also calculated how well each filter would

have "responded" to a sinusoidal grating of optimal spatial frequency, orientation and spatial phase, and of known Michelson contrast (see Eq. (2)). The ratio of grating contrast to the response of a filter to its optimal grating, was used as the scaling factor by which each point in the contrast "images" was converted to an *equivalent Michelson contrast*, ρ.

For each point in each image, and for each filter, the equivalent Michelson contrast was calculated. Due to the nature of the fast Fourier transform, however, this contrast image contained edge effects, and so only the central 158×158 points were included in our final distributions of natural-image contrasts. These 158×158 (pixels) $\times 64$ (filters) $\times 64$ (images) contrast values were placed in logarithmic bins to give a single histogram of the distribution of contrasts within our image set for each of the filter bandwidths. Any negative values were made positive, as if they had been the positive responses from simple cells with complementary receptive-field organisation.

2.6. Normalised contrast in images

In order to model contrast normalisation in striate cortex (cf. Heeger, 1992a, 1992b; Marr, 1970), the contrast response of each filter at each point in the image was also normalised according to the local averaged squared responses of the full set of 64 filters:

$$\rho_{i,\mathrm{norm}} = \frac{\rho_i}{\sqrt{k_i \sum_{i=1}^{64} \bar{\rho}_i^2}} \tag{11}$$

$\rho_{i,\mathrm{norm}}$ is the equivalent normalised contrast at a point in the image for a particular filter; ρ_i is the non-normalised contrast response of that filter to the image; and k_i is a constant for each filter, such that the normalised response of that filter to a sinusoidal grating of optimal spatial frequency, orientation and phase is equal to 1. The *normalising signal* (the divisor in Eq. (11)) is made up of terms $\bar{\rho}_i^2$, each of which is the contrast energy in the ith filter averaged over some area in the image. We tried different spatial extents of the averaging, with very similar results; we report the results of convolving the contrast energies in each filter by a two-dimensional Gaussian with spread of 17 pixels (the same Gaussian as used to make the 1.5 octave Gabor filter with carrier frequency 6 cycles per image). Brady and Field (2000) also modelled contrast normalisation; they used quadrature pairs of odd- and even-symmetric filters, and combinations of these would effect some spatial "blurring". Note that the square of $\rho_{i,\mathrm{norm}}$ in Eq. (11) would represent normalised contrast *energy*, and that addition of a term analogous to c_{50} would give us Heeger's version of Eq. (1). Only the filter set with 1.5 octaves spatial frequency bandwidth was used in these calculations, i.e. those filters most similar to mammalian striate cortex neurons (De Valois, Albrecht, et al., 1982; De Valois, Yund, et al., 1982; Movshon et al., 1978; Tolhurst & Thompson, 1981). Our model of normalisation assumes that neurons of all spatial frequencies and all orientations contribute equally to the normalising signal, and that the spatial spread of normalisation is independent of, say, orientation. In detail, these assumptions may prove to be inconsistent with neurophysiological studies (e.g. Walker, Ohzawa, & Freeman, 1999).

2.7. Mutual information

We also calculated the mutual information, $I(c;\hat{c})$, between the natural range of test contrasts, c, and the estimated contrasts, $\hat{c}$, as an alternative metric for the performance of the models. When calculating the mutual information, each stimulus contrast between 0.001 and 1.0 was simulated a number of times proportional to its estimated frequency of occurrence $P(c)$ in natural scenes:

$$I(c;\hat{c}) = \sum_{c} \sum_{\hat{c}} P(c;\hat{c}) \cdot \log_2 \frac{P(c;\hat{c})}{P(c) \cdot P(\hat{c})} \tag{12}$$

3. Results

3.1. Accuracy of contrast identification by single neurons

We simulated a large number of presentations of a range of contrasts to single neurons. A neuron's mean response to each contrast was first calculated, according to the Naka–Rushton equation (Eq. (1), Section 2). Then, for each trial, a neuronal response was sampled from a distribution modelled with variance roughly equal to twice the mean, and this integer response was used to make a Bayesian maximum a posteriori estimate of the presented contrast (Eqs. (3)–(6), Section 2). This estimate was based on the assumption that all contrasts were presented with equal probability. The difference between the estimated and presented contrasts was used to give a measure of the accuracy of the model's contrast prediction. Accuracy was defined as the inverse of the mean squared difference between the logarithms of estimated and presented contrasts, averaged over all trials for that contrast (Eq. (7)).

Fig. 2 shows the general form of graphs of the performance of single neurons in the simulated contrast identification task, calculated as *accuracy* by our model. The two curves correspond to two different $R_{\max}$ values (50—triangles; and 180—diamonds), for neurons with the same c_{50} (0.1) and an exponent, q, of 2. They show a central peak of accuracy at a slightly lower contrast than the neurons' c_{50}, flanked by two regions of much lower, approximately uniform accuracy. There is also an in-

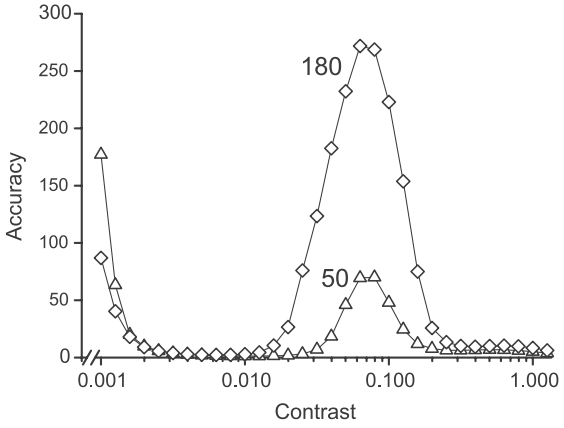

Fig. 2. Accuracy of contrast identification by single model neurons. Symbols represent the contrast identification performance (accuracy) of single neurons with R_{max} of 50 (triangles) and 180 (diamonds). Both neurons have c_{50} values of 0.1 and q values of 2. Both reach a peak at a similar contrast value, slightly below c_{50}, and also show an increase of accuracy towards the lowest contrast in the range. Data represent accuracy calculated over 10,000 trials.

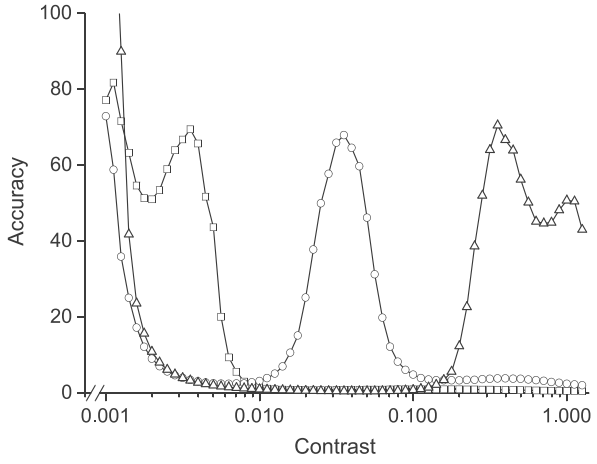

Fig. 3. Effect of changing c_{50} on contrast identification accuracy of single modelled neurons. Symbols show the contrast identification performance (accuracy) of single neurons with c_{50} values of 0.003 (squares), 0.03 (circles) and 0.3 (triangles). For all neurons, R_{max} was 50 and q was 2. Data represent accuracy calculated over 10,000 trials. For each neuron, the peak in accuracy occurs at just below the c_{50} value for that neuron. All neurons demonstrate an increase in accuracy towards the lowest contrast in the range; the size of this increase is greatest for the neuron with highest c_{50}, intermediate for that with lowest c_{50}, and lowest for the neuron with medium c_{50}. For the neuron with a c_{50} of 0.3 there is also an increase in accuracy at the upper end of the contrast range, which is not evident for the other neurons.

crease in accuracy towards the lowest contrast modelled. This low-contrast increase was a consequence of using a minimum contrast (resulting from our inability to represent zero on a logarithmic scale) in our contrast distribution. In our model, if a neuron produced a response of zero to the presented contrast, the estimated contrast was always the lowest contrast in our range (i.e. $P(c|r) = 1$ for $c = 0.001$ and $r = 0$). Thus, for low contrasts, where neuronal responses were most often zero (see Fig. 1A(i)), accuracy varied almost entirely according to the difference between the presented contrast and the lowest possible contrast. This effect was more prominent for the neuron with the lower R_{max}, (triangles), since this neuron would have a high probability of giving a response of zero for a wider range of contrasts than would the neuron with higher R_{max}. The effect of changing R_{max} on maximum accuracy will be shown in more detail in Fig. 5.

This ''artefactual'' rise in accuracy at the lowest modelled contrast results from the use of a continuous function like the Naka–Rushton function (Eq. (1)); zero is only finally attained at a contrast of zero. We experimented by applying a hard-threshold to the function, such that any response less than, say, 2% of R_{max} would be set to zero. This had the effect that many low contrasts would now have been equally likely to have evoked a response of zero; we then had to ''guess'' which of those many contrasts had been presented. The only effect of this was to spread the artefactually accurate guesses of low contrasts over a wider range. There was no effect on any other features of our results.

Fig. 3 shows how changing the parameter c_{50} affects the accuracy of a modelled neuron's identification of contrast, while keeping R_{max} constant at 50. Again, the exponent, q, was 2. The peak value of accuracy is independent of c_{50}, while the position of the accuracy peak along the contrast axis is consistently close to but, interestingly, slightly below the neuron's c_{50} (cf. Geisler & Albrecht, 1997). The contrast at which accuracy is a maximum corresponds neither to the steepest gradient of the contrast-response function along a linear contrast dimension nor along a logarithmic contrast dimension. The low-contrast artefact is also evident here, and is largest for the neuron with the highest c_{50} value (triangles), where the probability of getting a response of zero is higher than for the other neurons at all contrasts, and is particularly high at low contrasts. An additional feature is also evident at high contrasts: as c_{50} increases, contrast identification accuracy increases towards the upper end of the contrast range, a consequence of there being a maximum contrast. This is only evident at high values of c_{50}, where saturation has not been reached; any high value of response is interpreted as coming from the highest contrast available.

Fig. 4 shows the effect of changing the exponent, q, of the single neuron contrast-response function, where R_{max} is 10 and c_{50} is 0.1. Fig. 4A demonstrates that, as q is increased, so is the gradient of the contrast-response function for single neurons with identical R_{max} and c_{50} values. The increasing gradient is translated into an increase in peak contrast identification accuracy (Fig. 4B) from an exponent of 0.5 (squares) to 2.5 (diamonds), such that the relationship between the maximum accuracy and q is a steep straight line on log–log co-ordinates

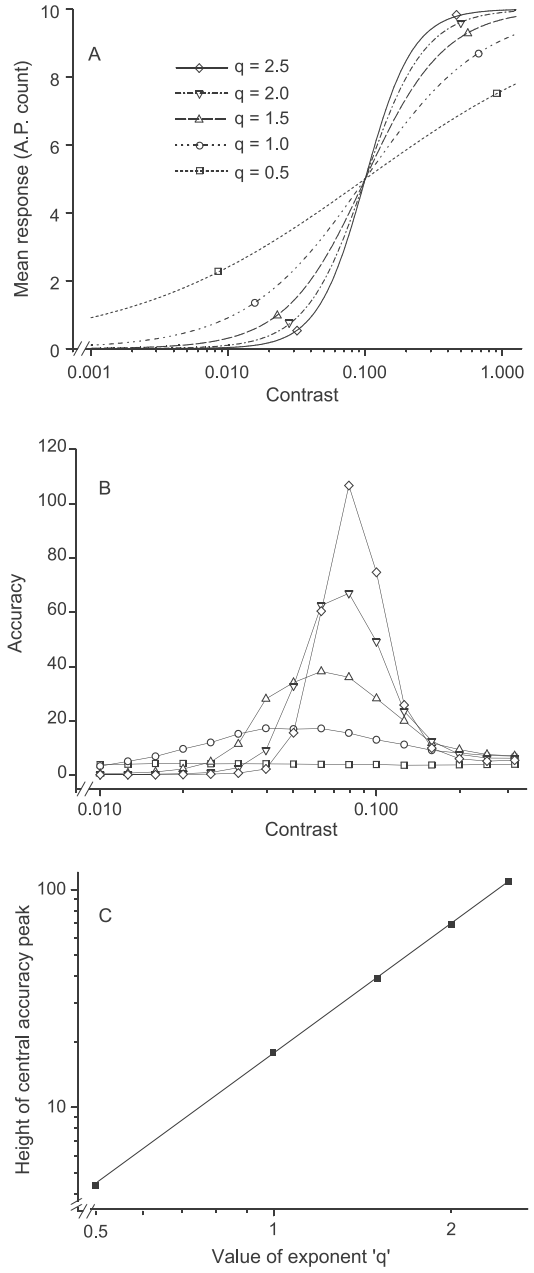

Fig. 4. Effect of changing contrast-response function exponent, q, on contrast identification accuracy of single modelled neurons. (A) Naka–Rushton contrast-response functions for single neurons with exponents, q, of 0.5 (squares), 1.0 (circles), 1.5 (upright triangles), 2.0 (inverted triangles) and 2.5 (diamonds). R_{max} is 50. As q increases, the gradient of the function increases, and the range of contrasts over which the neuron's mean response changes dynamically decreases. (B) Accuracy of contrast identification of neurons with identical q values to those shown in (A), Accuracy was calculated over the contrast range 0.001–1.26; results of calculations over the restricted range 0.01–0.32 are shown. Increasing q increases the peak accuracy of a single neuron while reducing the range of contrasts that can be identified with more than baseline accuracy. Accuracy is shown over a restricted range of contrasts, in order to avoid showing the low-contrast artefact, which has already been described. This is also the case for Fig. 5. (C) Scatter plot of the relationship between q and peak contrast identification accuracy. This relationship is a straight line on log–log co-ordinates.

(Fig. 4C). Fig. 4B also shows that as q increases, the accuracy curve narrows. This makes intuitive sense because, as the gradient increases for the same R_{max}, the range of contrasts over which the response changes significantly must narrow. The area under the accuracy profile changes rather little.

3.2. Populations of neurons

Populations of neurons were modelled by calculating the Bayesian posterior probability distribution $P(c|r_i)$ for each neuron, and combining these probability distributions in a way that retained the information provided by the differential responses of individual neurons (Section 2, Eq. (8)). The model's estimate of contrast was that at which this overall probability distribution $P(c|\mathbf{r})$ was a maximum. This is the first of the two models described in the Section 2. The second model is discussed later in this section.

Fig. 5 compares the effect of changing R_{max} for a single neuron with the effect of changing the number of neurons in this model, each with identical R_{max}. All neurons had identical c_{50} and q values (0.1 and 2 respectively). Accuracy increases with R_{max} (Fig. 5A), and in an identical manner with number of neurons (Fig. 5B). To change the maximum accuacy, therefore, requires only a change in the *product of* R_{max} *and number of neurons*, i.e. the total number of action potentials generated on average (Fig. 5C); for a given accuracy, there is a simple trade-off between the number of neurons and the response amplitude of individual neurons. The dotted line has a gradient of 1, and provides a good fit to the results.

Accuracy of contrast identification was also calculated for populations of neurons with c_{50} values taken from neurophysiological single neuron studies in cat (Tolhurst, unpublished; see figure legend), and we were generously provided with numerous and detailed data for *macaca fascicularis* by Ringach, Hawken, and Shapley (personal communication) (see e.g. Ringach, Hawken, & Shapley, 1997). Fig. 6 shows the full distributions of c_{50} values for these populations of 138 cat neurons (Fig. 6A; median 0.11) and 219 macaque neurons (Fig. 6B; median 0.21). These distributions of c_{50} are consistent with other studies (e.g. Anzai, Bearse, Freeman, & Cai, 1995; Geisler & Albrecht, 1997; Sclar et al., 1990; Sengpiel, Baddeley, Freeman, Harrad, & Blakemore, 1998) although these monkey data are less weighted to high contrasts than those of Sclar et al. (1990). All neurons were modelled with an R_{max} value of 10 and exponent, q, of 2, and both populations consisted of eighteen neurons, sampled at uniform intervals from the populations arranged in ascending order of c_{50} value, except that we did not include any of the monkey

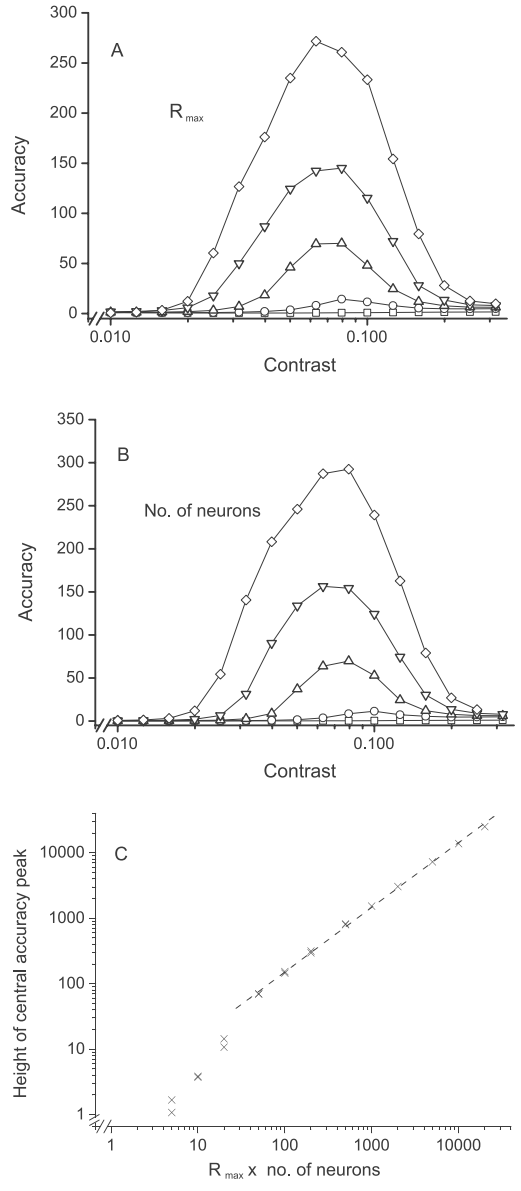

Fig. 5. Effect of changing maximum response, R_{max}, and number of neurons, n, on contrast identification accuracy. (A) Effect of changing R_{max} on contrast identification accuracy of single neurons with q of 2 and c_{50} of 0.1. Results of calculations are shown over the restricted range 0.01–0.32. R_{max} values are 5 (squares), 20 (circles), 50 (upright triangles), 100 (inverted triangles) and 180 (diamonds). Increasing R_{max} increases the contrast identification accuracy of single neurons at all contrasts, most obviously the peak accuracy, without changing the contrast at which accuracy is a maximum. (B) Effect of changing n on contrast identification accuracy of single neurons with R_{max} of 5, q of 2 and c_{50} of 0.1. Results of calculations are shown over the restricted range 0.01–0.32. n values are 1 (squares), 4 (circles), 10 (upright triangles), 20 (inverted triangles) and 36 (diamonds). Increasing n, like increasing R_{max}, increases the contrast identification accuracy of single neurons at all contrasts (most obviously the peak accuracy), without changing the contrast at which accuracy is a maximum. (C) Scatter plot of the relationship between the product of R_{max} and n, and peak contrast identification accuracy. For values of this product above approximately 20, the relationship is a straight line on log–log co-ordinates with a slope of 1.

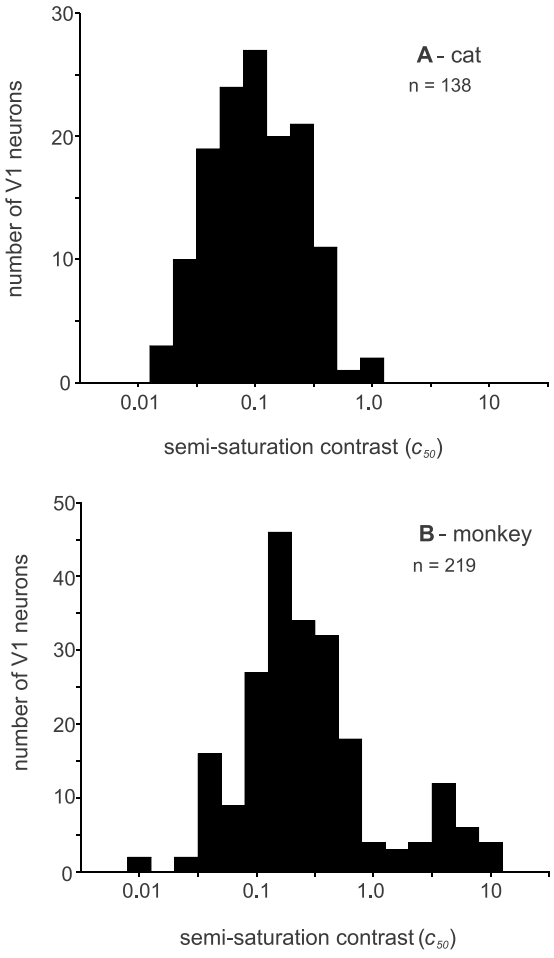

Fig. 6. Distributions of c_{50} in modelled populations. Histograms of c_{50} values from single neuron recordings in striate cortex. (A) Cat (Tolhurst, unpublished): values from all 138 neurons are shown, in logarithmic bins. The distribution median was 0.11. The data are from a variety of studies including (Dean, 1981a; Dean & Tolhurst, 1986; Tolhurst et al., 1983; Tolhurst & Dean, 1990, 1991). (B) *Macaca fascicularis.* Generously given to us by Ringach, Hawken, and R. Shapley (personal communication) (see e.g. Ringach et al., 1997). Values from all 219 neurons are shown, in logarithmic bins. Semi-saturation contrast values above 1.0 (30 neurons) were not sampled in our models. Median c_{50} of the sampled 189 neurons 0.18.

data with c_{50} above 1. The rationale for this was that the high c_{50} neurons differed with respect to other response parameters, and so could not be seen as part of a homogenous neuronal population (see Section 4).

Fig. 7 shows the contrast identification performance of these two modelled populations of neurons. The symbols show the calculated accuracy for cat (triangles) and monkey (squares) neurons. Both curves are noticeably wider than for single neurons with contrast-response functions with an exponent of 2 (compare Fig. 2). The curve for the population of cat neurons (triangles) lies to the left of that for the monkey neurons (squares), i.e. the cat model performs better at lower

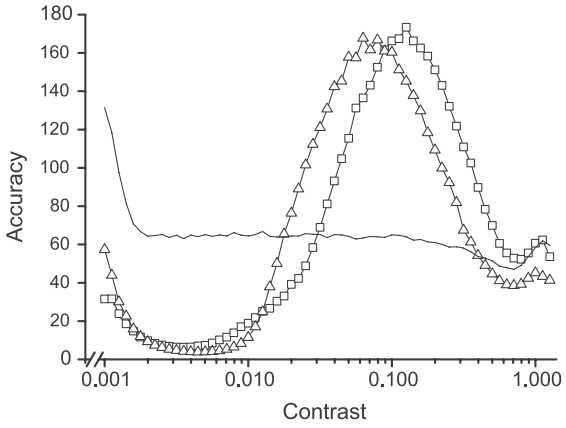

Fig. 7. Accuracy of contrast identification for models of realistic neural populations. Symbols show contrast identification accuracy for sets of eighteen neurons with c_{50} values sampled at uniform intervals from population data in cat (triangles; Fig. 6A) and monkey (squares; Fig. 6B), arranged in ascending order of c_{50} value. The line without symbols shows contrast identification accuracy for an imaginary population of eighteen neurons, with c_{50} values at uniform intervals of logarithmic contrast along the range 0.001–1.26. The peaks in the distributions are a result of the non-uniform distributions of c_{50} values; the equally spaced c_{50} data (line without symbols) are equally accurate across the range of contrasts, with the exception of small increases in accuracy at the lowest and highest contrasts.

contrasts than the monkey model, and the latter performs better at higher contrasts, as would be expected from the differences in median c_{50}. The peaks of the accuracy curves are positioned slightly below the median values of the c_{50} distributions.

The curve without symbols corresponds to a population of an equal number of neurons (18), again with identical R_{max} (10) and exponent q (2), but with sigma values distributed in equal logarithmic steps along the whole contrast range in our model. In this case there is no central accuracy peak, but the artefactual peaks at low and high contrasts are evident.

3.3. The contrasts in natural images

Contrasts in a set of 64 natural images were calculated as the Michelson contrasts of sinusoidal gratings producing equal responses in a set of Gabor filters to those produced by the images (see Section 2). We used three sets of Gabor filters, with spatial frequency bandwidths of 1.0, 1.5 and 2.0 octaves, and corresponding orientation bandwidths of 22°, 36° and 48° (half-width at half height). Fig. 8A shows the distribution of contrasts calculated in our set of images, for the three different bandwidths of Gabor filters. Each of the three filter sets gave a distribution following a similar bell-shaped curve, but broadening the filters' bandwidth had the effect of shifting the distribution to the right, i.e. to higher equivalent contrasts. The broader-band filters "see" more energy in their passband than do the nar-

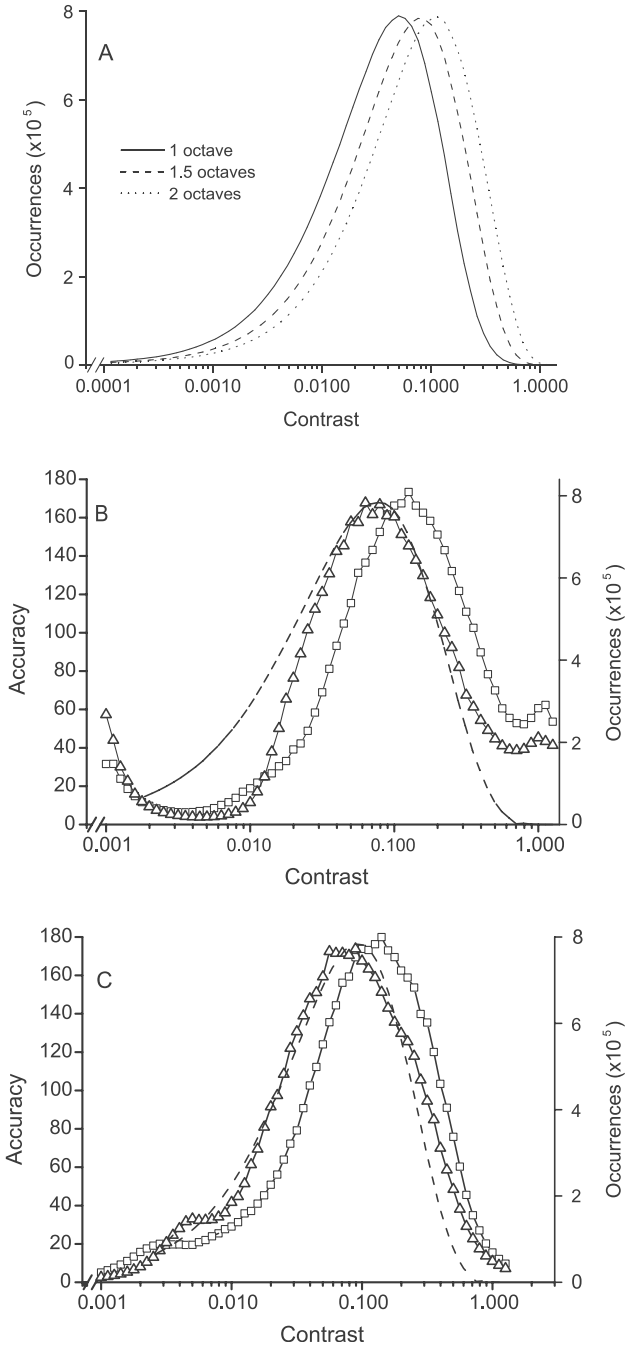

Fig. 8. Comparison of population contrast identification accuracy and the distribution of contrasts in natural images. (A) Calculated distributions of contrasts in a set of 64 natural images. Distributions are shown for 3 separate sets of 64 Gabor filters; the 3 sets had spatial-frequency bandwidths of 1 octave (solid curve), 1.5 octaves (dashed curve) and 2 octaves (dotted curve), and orientation bandwidths of 22°, 36° and 48°, respectively (half-width at half height). (B, C) Symbols show contrast identification accuracy for populations of 18 neurons from cat (triangles; Fig. 6A) and monkey (squares; Fig. 6B), assuming (B) that all contrasts were equally likely to have been presented in the simulated contrast identification task, and (C) using the distribution of contrasts in natural images (for filters of 1.5 octave spatial-frequency bandwidth) as *a priori* knowledge of the probability of each contrast being presented $P(c)$. The dashed curve shows the distribution of natural image contrasts calculated using filters with 1.5 octave spatial-frequency bandwidth (dashed curve in (A)).

rower filters—hence, the calculated contrast is higher for the broader-band filters.

In making a comparison between population accuracy of contrast identification and the distribution of natural image contrasts, we used two methods for calculating accuracy. First, as previously, accuracy was calculated assuming that $P(c)$ (Eq. (5)) was the same for each of the contrasts in our range (Fig. 8B is the same as Fig. 7). To compare this with the contrasts in the natural world, we chose to compare with Gabor filters with bandwidths of 1.5 octaves and 36°, because these are most similar to the mean values for *real* cortical neurons (e.g. De Valois, Albrecht, et al., 1982; De Valois, Yund, et al., 1982; Tolhurst & Thompson, 1981). The dashed line in Fig. 8B (re-plotted from Fig. 8A) is the distribution of contrasts in natural images as measured with filters of 1.5 octaves bandwidth. The accuracy of contrast encoding by the population of cat neurons (triangles) follows the distribution of contrasts in natural images very closely: the neurons are most accurate at encoding the contrasts that occur most often. The accuracy of encoding by monkey neurons (squares) appears to be a poorer match to the contrasts in natural images.

Second, in making a decision about the presented contrast from neuronal responses, the brain may be influenced by *a priori* knowledge of how often different contrasts occur in natural scenes. Thus, instead of using a uniform $P(c)$, we can make $P(c)$ the same as the probability of occurrence of different contrasts (the dashed curve of Fig. 8A in the range of contrasts 0.001–1.26). Fig. 8C shows the calculated accuracy of contrast identification for the populations of 18 cat neurons (triangles) and 18 monkey neurons (squares) when the prior probability is determined by the frequency of occurrence of contrasts in our set of 64 natural images as calculated with the 1.5 octave Gabor filters. The major effect is that the accuracy curves become more unimodal, and the "artefacts" at very low and very high contrasts are removed; these very low and very high contrasts are unlikely to occur and so they are rarely chosen from the neuronal responses. Instead, there is a small mode at moderate to low contrasts. With the prior probabilities taken into account, the encoding by the cat population (triangles) resembles the distribution of natural contrasts calculated with 1.5 octave Gabors even more closely (dashed curve), but the curve for the monkey population is still slightly offset.

3.4. Contrast estimation using an alternative model of neural pooling

A second model for pooling of neuronal responses was used to calculate contrast identification accuracy, where information from the differential firing of single neurons was *not* accounted for (cf. Boynton et al., 1999; Britten et al., 1992; Heeger et al., 2000). Rather, the total summed activity in the population of neurons was used in the estimation of contrast (Section 2, Eqs. (9) and (10)). We show only the results for the cat model since the monkey model produced a similar effect. On each trial at each contrast, the responses of the 18 neurons were drawn from the appropriate probability distributions, and these 18 responses were simply summed before a contrast estimate was made.

Fig. 9A shows the contrast-response function for the summed population responses of cat neurons. The

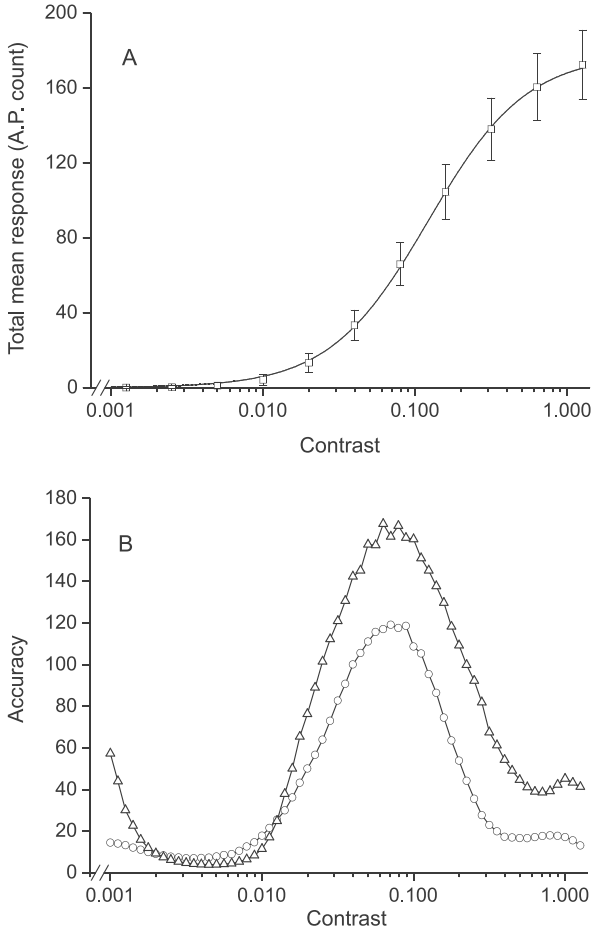

Fig. 9. Contrast identification accuracy using an alternative response-pooling model. (A) Population contrast-response function, for a population of 18 neurons, based on data from cat (Fig. 6A). Symbols show the mean total response of the 18 neurons, with error bars which are the square roots of the response variance, calculated from 1 million simulated presentations of each contrast. The curve is the best fit of the Naka–Rushton equation to the total mean population response. The parameters of this fit were: $q = 1.34$, $R_{max} = 178$, $c_{50} = 0.121$. This curve approaches saturation at the highest contrasts. (B) Contrast identification accuracy for two models of neural pooling, both using 18 neurons based on the data from cat. The first model (triangles) accounts for the differential activity of all the neurons in the model, while the second (circles) accounts only for the difference in total firing rate of the 18 neurons. The peak accuracies of the first (differential activity) model exceed those of the second (total activity) by a factor of approximately 1.61.

symbols in the graphs show examples of means and standard deviations of summed responses after 1 million trials (the simulation was actually done over 311 contrasts). The solid line is the best fitting Naka–Rushton function. It is similar in form to those for individual neurons but with shallower slope (see figure legend). The increase in response variance of individual neurons with increasing firing rate is reflected in the variance of the population response, which is twice the population mean response. In the simulation of Fig. 9B, it made no difference whether we simulated the responses of the 18 model neurons and then summed them, or whether we modelled a single neuron whose contrast-response function was the best fit to the results of Fig. 9A.

Fig. 9B compares contrast identification accuracy for modelled populations of cat neurons, for both models of neuronal pooling, assuming a uniform $P(c)$. The triangles show the results for the first pooling model, redrawn from Fig. 8. The contrast identification accuracy based on the summed population responses is shown as circles. The contrast at which the accuracy peak occurs does not vary between models, but peak accuracy is greater when the *differential activity* of individual neurons is accounted for (triangles). Overall, in the contrast range 0.01–1.0, the area under the triangles is 1.61 times greater than that under the circles. The same proportionate difference in accuracy for the two models was found when we modelled populations with 10, 18, 28 or 35 neurons. We also examined the effect of a "hard threshold" (see Section 2); this slightly exaggerated the difference between the two pooling models.

3.5. Histogram equalisation

The match between encoding accuracy and the distribution of natural contrasts (Fig. 8), implies some form of "histogram equalisation" of responses (Laughlin, 1981). This means that all equally discriminable steps in response level will be used with equal frequency. Fig. 10A plots the cumulative probability of occurrence of different natural contrasts (solid curve), and the population response of the 18 model cat neurons (dashed curve) is redrawn from Fig. 9A. The two ordinates are scaled arbitrarily against each other. The match between the two curves is poor, much poorer than those for fly neurons (Laughlin, 1981) or for most kinds of cat and monkey retinal and LGN cells (Tadmor & Tolhurst, 2000). This mismatch is not surprising since the multiplicative dependence of response variance on average response magnitude in cortex means that equal increments of response magnitude will not signal increased contrast with equal reliability.

In Fig. 10B, the cat population responses are transformed so that equal steps *are* almost equally reliable, i.e. each step approximates to a fixed number of d' units. This can be *approximated* (except at the very lowest response levels, perhaps) by dividing each response by the standard deviation of that response (strictly, by the square root of the variance); since variance is proportional to mean, this is equivalent to taking the square root of the response itself. The transformed response curve (dashed curve in Fig. 10B) *does* give a passable match to the cumulative distribution of natural contrasts (solid curve).

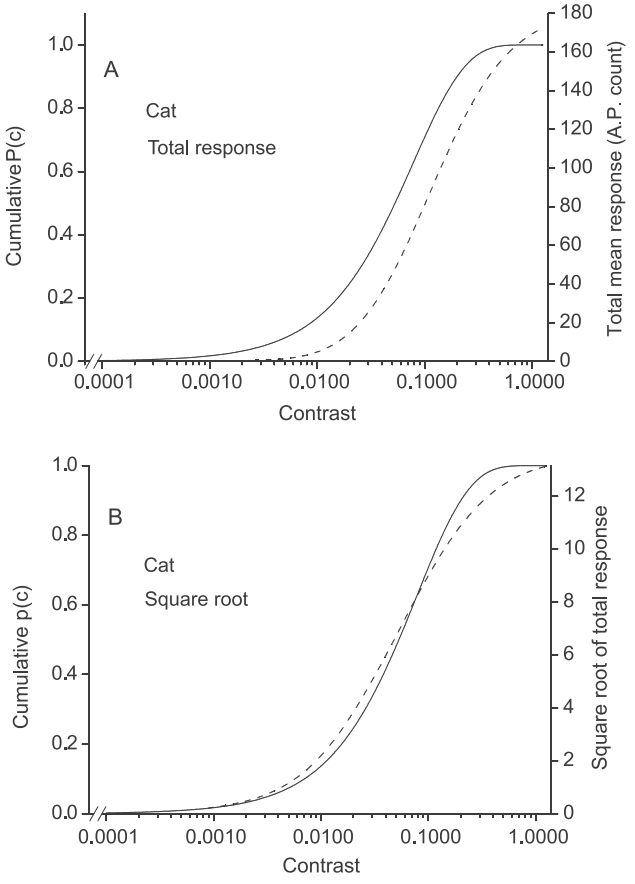

Fig. 10. Population responses and natural image contrasts. (A) The dashed curve shows the contrast-response function for a modelled population of 18 neurons, based on data from cat (Fig. 9A). The solid curve shows the cumulative distribution of contrasts in our set of 64 natural images, expressed as probability of occurrence, $P(c)$. The vertical scales are manually adjusted to give the best-fit possible. The two curves do not match. (B) The dashed curve shows the square roots of the mean responses to a range of contrasts from 0.0001 to 1.26, for the same population of 18 neurons as in (A). The distribution of square roots of the mean responses represents the cumulative distribution of discriminable steps in the total response. The solid curve shows the cumulative distribution of contrasts as shown in (A). The two curves match reasonably.

3.6. Contrast normalisation

Our analysis of the contrast in natural images implies that each neuron responds independently to features in its passband. However, it is widely believed that a neu-

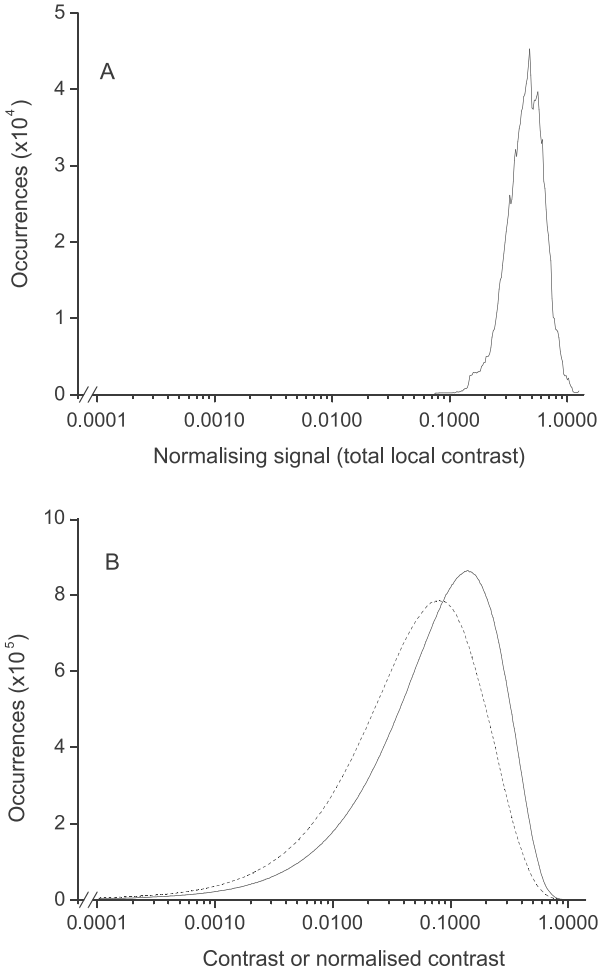

Fig. 11. The effect of contrast normalisation on the distribution of image contrasts. (A) The distribution of the normalising signal, i.e. the spatially weighted total contrast in the image, for our set of 64 natural images. The filters used in the calculation of the normalising signal had a spatial-frequency bandwidth of 1.5 octaves. The distribution is rather narrow along a logarithmic contrast dimension. (B) The solid curve shows the distribution of "normalised contrasts" in our set of 64 natural images (i.e. the contrasts calculated using independent filters of spatial-frequency bandwidth 1.5 octaves, divided by a spatially weighted average of the total local contrast, the normalising signal shown in (A)). The dotted curve shows the distribution of contrasts in natural images, calculated using independent filters of spatial-frequency bandwidth 1.5 octaves (Fig. 8A). The solid curve is slightly narrower than the dotted curve, and peaks at slightly higher contrast.

ron's response to such features will be influenced by the activity of neurons responsive to other features (e.g. Bonds, 1989; Heeger, 1992a, 1992b). There is a process of *contrast normalisation* whereby the response of each neuron is thought to be divided by the total contrast energy or the total response of the neuronal population. Thus, it is possible that a feature of given contrast in different natural scenes might evoke different responses from the population of neurons responsible for encoding that contrast, depending upon the presence or absence of other features. Differences in overall contrast energy in different natural scenes would lessen the accuracy of contrast coding in our simplified case.

We calculated the normalising signal as the total contrast at each point in each of the 64 natural images, by squaring the responses of each of the 64 Gabor filters (1.5 octave bandwidth), summing the squared responses; averaging the sum over an area of the image (see Section 2) and then square-rooting the averaged sum (Section 2, Eq. (11)). Fig. 11A shows the distribution of this normalising signal in the set of natural images. It is notable that the distribution is very narrow, implying that the summed contrast across all orientations and spatial frequencies varies rather little within and between natural images (Lauritzen & Tolhurst, 2000; Tolhurst et al., 1997). Fig. 11B shows the distribution of contrasts as estimated by *independent* Gabor filters (dotted curve, redrawn from Fig. 8) and the distribution of contrasts after normalisation (solid curve), calculated by dividing each contrast estimate by the value of the local normalising signal and a constant k (Eq. (11)). The distribution of normalised contrasts is slightly narrower than for the independent contrast estimates (Brady & Field, 2000), and the peak of the curve has moved to slightly higher contrasts. Normalisation has had little effect on the distribution of natural contrasts. We will consider the circumstances in which normalisation does have an effect elsewhere (Lauritzen & Tolhurst, 2000).

4. Discussion

In this paper, we have investigated how well populations of neurons in striate, primary cortex (V1) might encode the contrast of a simple stimulus. We have simulated a task in which an animal must estimate the contrast of a sinusoidal grating from the numbers of action potentials generated by one or more neurons in response to that stimulus. Our models allow that any one cortical neuron responds differentially over only a limited range of contrasts and that there is large trial-to-trial variability in the numbers of action potentials generated in response to identical stimuli. The estimated contrast is the one most likely to have evoked that pattern of responses from the several neurons (Geisler & Albrecht, 1997).

4.1. An ecological match to the contrasts in natural scenes?

We have demonstrated by computer modelling how stylised striate cortex neurons could contribute to contrast identification and how varying the parameters of a single neuron's contrast-response function would affect its potential for estimating contrast. Single neurons can allow accurate identification over only a limited range of contrast. However, the range of contrasts that can be

accurately identified is increased by pooling information from neurons with dynamic ranges covering different contrasts. In particular, we have compared two different pools of neurons, based on populations of neurons from neurophysiological studies in cat and monkey, and we have related the performance of the two pools in the simulated contrast identification task to the distribution of contrasts actually found in natural scenes.

Populations of neurons with contrast-response curves similar to those modelled would not allow uniform contrast identification accuracy across all possible contrasts. Instead, accuracy would be greatest at intermediate contrasts (Michelson contrasts of 0.05–0.3), and would fall considerably at lower and higher contrasts, especially if an animal's decisions included some *a priori* knowledge or experience of the non-uniform distribution of contrasts in the natural world. We have related the results of our simulations to the distribution of contrasts in natural scenes (Fig. 8), and have found that the contrasts best identified by neuronal populations based on data from cat and monkey studies are those most frequently found in natural scenes.

The close match of the accuracy profile to the distribution of contrasts in natural images implies an evolutionary or adaptive match: an optimisation of the visual cortex for encoding natural contrasts. But, in what sense is the encoding optimised? Table 1 summarises several performance measures for a variety of models that we have described that incorporate 18 neurons with R_{max} of 10 and q of 2. In fact the model giving the greatest accuracy at a single contrast consists of 18 neurons with identical c_{50} rather than the model based on realistic cat c_{50} values! The total area under the accuracy profile is rather similar for all models. So it seems that the height of the accuracy peak can be traded off against the range of contrasts over which the model performs well. We also calculated mutual information between actual and estimated contrast (Section 2, Eq. (12)) as a more recognisable metric of coding performance. The mutual information *is* greatest for the realistic cat model, but the superiority over the other models is not dramatic, so that the good match of the accuracy profile to the distribution of natural contrasts still demands a convincing metric. There is an important point: the model that notes the differential activity of different neurons conveys more information than the model that simply sums neuronal activity without discrimination.

However, the contrasts best identified by neuronal populations based on studies in monkey do not match natural scene contrasts as well. This may reflect the findings of Tadmor and Tolhurst (2000) who showed that retinal and LGN neurons in cat have contrast-response functions that closely match the cumulative distribution of contrasts in natural images, whereas only cells in the magnocellular pathway in monkey match this distribution. The contrast-response functions of monkey parvocellular cells show a poor match to the cumulative distribution of contrasts in natural images. In fact, some monkey cortical neurons have very high c_{50} values (Fig. 6B; Sclar et al., 1990) and we did not include any neurons with c_{50} above 1 in our models. Model neurons with high c_{50} and exponent q of 2 would produce very little response in the range of physically achievable contrasts (up to 1). This shows the limitations of our simplification that all neurons will have the same q and R_{max}. For example, neurons with high c_{50} are in fact likely to have had very shallow contrast-response functions in the achievable range of contrasts, and the high c_{50} results from extrapolation of the data beyond the measured range. A more realistic model of monkey visual cortex might include a more realistic acceptance that neuronal behaviours may vary and may not be stereotyped (Geisler & Albrecht, 1995, 1997). However, it is still the case that monkey c_{50} values tend to be higher than those of the cat, so that the cat and monkey models will not provide the same match to natural contrasts.

Perhaps the match between identification performance (especially in cat) and natural image contrasts results from experience of the natural contrasts to which the visual system is exposed. Whilst the maximum firing rates of individual neurons, and the numbers of neurons within a population, may affect overall contrast identification accuracy (see Fig. 5), it is primarily the neurons' c_{50} values that determine the contrasts at which identification will be most accurate (Fig. 3). Thus it seems that

Table 1
Three measures of coding performance for several model populations of neurons

	Peak accuracy	Area under accuracy profile	Mutual information (bits)
18 identical neurons, $c_{50} = 0.1$	282	3509	2.42
18 neurons, evenly spaced c_{50}	71	2468	2.23
18 cat neuron c_{50} values, pooling rule 1	167	3779	2.46
18 cat neuron c_{50} values, pooling rule 2	121	2354	2.16

All neurons had $R_{max} = 10$ and $q = 2$. The peak accuracy, the area under the accuracy profile between contrasts 0.01 and 1.0, the mutual information between estimated and actual contrast are shown. In the latter case, each contrast was simulated a number of times proportional to its occurrence in natural scenes. Pooling rule 1: the differential activity of different neurons is taken into account. Pooling rule 2: the activity of the 18 neurons is simply summed before a decision is made. Graphs for the four models are shown in Fig. 5B (triangles), Fig. 7 (line without symbols), Fig. 7 (triangles) and Fig. 9 (circles) respectively.

evolution or developmental plasticity of the visual system (or a combination of the two) has caused the c_{50} values of the visual system's neurons to become matched to the contrasts it encounters. We are not aware of any studies that have measured contrast-response functions of neurons throughout their development, and so it is not yet clear whether their c_{50} values change throughout their lifetimes (suggesting plasticity in visual cortex) or whether they are fixed (suggesting a purely evolutionary basis for our findings). It is still an important question why monkey cortical neurons (and P-cells in more peripheral pathways) are not as well matched to the task of luminance contrast identification.

Perhaps, the cat and monkey neurons perform better over slightly different contrast ranges because the cat is nocturnal and the monkey is diurnal. At the light levels generally used for laboratory experiments, the monkey might be at a lower level of light adaptation compared to the cat, but with the capacity to have increased contrast sensitivity at higher light levels. In direct sunlight, the contrasts in the natural world are some 15% higher than in diffuse illumination because of the added contrast of the highlights and shadows cast in direct light (Lauritzen & Tolhurst, 2000). Perhaps, a diurnal lifestyle is met more often with direct, "shadowy" illumination whilst a nocturnal lifestyle is met more often with diffuse, "flat" illumination. The selection of photographs from which we estimated the distribution of contrasts in natural scenes included images of direct and diffuse illumination.

The monkey's visual system with its smaller receptive fields is responsive to higher spatial frequencies than the cat's. This might contribute to any difference in the level of light adaptation in the retina. It is also possible that the different contrast sensitivity of V1 neurons matches a difference in the contrasts of high and low spatial frequencies in natural scenes. However, the Fourier spectra of natural scenes fall off steeply with spatial frequency (Tolhurst et al., 1992), more steeply than can be compensated for with neurons of fixed logarithmic bandwidth (Field, 1987). The puzzle of the low sensitivity of monkey neurons remains and it may be resolved when any conflicting constraints on the *dual* role of P-cells in coding colour as well as luminance information are better understood.

We propose that the population contrast-response properties of cat cortical neurons particularly suit them to the task of encoding naturally encountered contrasts. In fact, there is no straightforward definition of contrast in a complex image (Field & Brady, 1997; Peli, 1990; Tadmor & Tolhurst, 1994). Contrast is a measure of luminance modulation divided by a measure of local mean luminance, and a pragmatic definition of contrast must match the receptive-field properties of the neurons under consideration. The magnitude of the contrast of a feature in a natural scene depends upon the bandwidth of the "operator" (the receptive field model) used to calculate it (see Fig. 8A). The spatial-frequency and orientation bandwidths vary considerably between striate cortex neurons, and there tends to be a systematic variation of spatial-frequency bandwidth with the optimal spatial-frequency (e.g. Baker, Thompson, Krug, Smyth, & Tolhurst, 1998; De Valois, Albrecht, et al., 1982; De Valois, Yund, et al., 1982; Tolhurst & Thompson, 1981). Accounting for differences in spatial-frequency and orientation bandwidth might slightly alter our conclusion about how well cortical neurons are matched to encoding natural contrasts, but it is unlikely that this would account for the slight mismatch of monkey cortical neurons.

Our interpretation has not accounted fully for the phenomenon of *contrast normalisation* (Heeger, 1992a, 1992b) where the response of one cortical neuron to a given contrast is affected by the presence of contrasts at other spatial frequencies or orientations. If a given feature is presented in many different contexts in natural scenes, it may evoke different responses at different times. Hence, a simple contrast identification task will be subject to error, unless the task is reformulated to be one of identifying the *normalised* contrast instead of contrast per se. This is similar to Marr's (1970) proposal that the responses of a cortical neuron encode the probability that the stimulus consists entirely of its own "trigger feature"; a high firing rate can never be evoked by a non-optimal stimulus, even if it is of very high contrast (Geisler & Albrecht, 1995). In fact, we have found in our sample of digitised photographs of natural scenes that the total contrast energy (the normalising signal) does not vary much within and between scenes (Fig. 11A), and so we believe that the difference between identifying contrast and normalised contrast in natural scenes will not be very great.

4.2. Models of neuronal response and of response pooling

In detail, the predictions of our models depend on the validity of our assumptions about the responses of striate cortex neurons to contrast. The Naka–Rushton equation has been established as a close description of an individual neuron's contrast-response function (Albrecht & Hamilton, 1982; Gardner et al., 1999; Sclar et al., 1990; Tolhurst & Heeger, 1997). Although the exponent, q, is perhaps not always equal to 2, there is a sound basis for modelling a value of 2 (e.g. Heeger, 1992a, 1992b), with the exception of, perhaps, neurons with very high c_{50}s. The exact values taken in our model by the maximum response rate, $R_{\max}$, and the number of neurons, n, are not important for the interpretation of our present results, as we claim only to evaluate the *relative* contrast identification performance of different models. Our particular choice of 18 neurons with an $R_{\max}$ of 10 was guided by attempts (Chirimuuta et al., in

preparation) to fit the exact form of the experimentally measured "dipper function" for contrast discrimination (e.g. Legge & Foley, 1980). We have generally modelled small values of R_{max} since cortical neurons often do not generate very high firing rates in response to their optimal stimuli and, in the 100–200 ms that one might reasonably allow for a perceptual decision, a total action potential count of only 10 is not unreasonable (Geisler & Albrecht, 1997; Sclar et al., 1990; Smyth, Willmore, Thompson, Baker, & Tolhurst, in press). In our experience of cat cortex, it is only special complex cells (Gilbert, 1977) that have high firing rates.

We have found some evidence for a correlation between R_{max} and c_{50} in the population of cat neurons (Tolhurst, unpublished), but this is not strong, and we have found the effect on our model to be small. There might also, of course, be other correlations between, say, c_{50} and q (see our discussion of the monkey neurons with very high c_{50}), or between the parameters of the Naka–Rushton fit and other neuronal parameters such as noise amplitude, optimal spatial frequency or tuning bandwidth. The exact behaviour of a real set of neurons could only be seen in detail by modelling each neuron's exact properties (Geisler & Albrecht, 1997); one would have to ensure that the neuronal sample is a fair sample of those neurons contributing to perception and that the population parameters are not affected by samples of, say, interneurons or corticothalamic neurons, whose properties may be different. Our modelling is based on stylised neurons so that we can examine the different contributions of different neuronal properties.

We have used a two-stage Poisson model to simulate the trial-by-trial variance of neuronal responses. This gives the desired result that variance is twice the mean response, and it also produces response distributions that look realistic (cf. Tolhurst, 1989). A Gaussian noise model would be very unrealistic at the low mean firing rates that we believe are appropriate to the model. We have taken the simplistic view that the response of a single neuron to a single stimulus trial can be represented as an action-potential count. It may be that the exact timing of action potentials in the responses of real neurons may convey some extra information (e.g. Reich, Mechler, & Victor, 2001).

In considering how a population of neurons could combine to encode a wide range of contrasts, we have compared two ways of pooling the information provided by the individual neurons in the population. One of the simplest pooling rules would be to sum the action-potential counts of the neurons in the population, discarding any specific information regarding which neurons gave which response (cf. Britten et al., 1992). Indeed, in the present simulations, the pool of 18 different neurons behaved just like a single neuron with shallower contrast-response function and higher firing rate. This pooling model has the attraction that such a population response might actually be measurable with, say, fMRI where it is argued that the BOLD signal may be proportional to the population action potential count (Boynton et al., 1999; Heeger et al., 2000). However, it has recently been argued that the BOLD signal relates more to synaptic potentials than to action potentials (Logothetis, Pauls, Augath, Trinath, & Oeltermann, 2001). But a simple pooling of responses begs the question why the cortex should have neurons with limited dynamic ranges that need to be pooled, when the earlier stages of the visual pathway have neurons whose responses cover the whole range of natural contrasts.

The more complicated pooling rule takes into account the differential firing of the different neurons by estimating contrast from *knowledge of how each neuron's responses depend on contrast* (Geisler & Albrecht, 1997). The accuracy of contrast identification would obviously be higher if the responses of individual neurons were interpreted separately, rather than just being indiscriminately summed (Fig. 9). However, the simple pooling model is not greatly inferior. Given the simple trade-off between the number of neurons in the models and their maximum firing rates (Fig. 5), we can easily imagine that any deficiency of the simple pooling rule could be overcome if the number of neurons in the pool were increased by about 60%. This is true, at least, for the task that we are simulating in this paper: the accurate identification of the contrast of a single stimulus presentation. It will be interesting to discover whether there may be other tasks, such as contrast discrimination or masking, where the predictions of the simple and complex pooling rules are more different.

4.3. Histogram equalisation and sparse responses

The population of cat cortical neurons encodes contrasts most accurately when they are similar to those found in natural scenes. The cumulative distribution of contrasts in natural scenes is not a particularly good match to the population contrast-response function, but it does match the way in which *equally discriminable* response steps (equivalent to d' steps) increase with contrast. This is analogous to a form of histogram equalisation (Laughlin, 1981), implying that the non-uniform distribution of natural contrasts will map into a uniformly spaced distribution of equally reliable responses. Thus, the code for contrast will have maximum entropy. However, this seems to imply that response states evoking many action potentials would be about as likely as states evoking few, and it has been estimated that the generation of action potentials in cerebral cortex may be costly (Attwell & Laughlin, 2001; Levy & Baxter, 1996). It has been argued that the cortex might sacrifice the ideal of a maximum-entropy code in order to minimise the energy costs of action potential generation, so that the use of high firing rates would be

minimised (Baddeley et al., 1997; Balasubramanian, Kimber, & Berry, 2001). An energy-efficient contrast code would show a non-uniform distribution of response states. Experimental studies of single cortical neurons (Baddeley et al., 1997; Smyth et al., in press; Vinje & Gallant, 2000) and theoretical studies (e.g. Bell & Sejnowski, 1997; Field, 1994; van Hateren & van der Schaaf, 1998; Hyvarinen & Hoyer, 2001; Olshausen & Field, 1997; Ruderman, 1994; Willmore & Tolhurst, 2001) suppose that the responses of cortical neurons to natural scenes should be highly *non*-uniform.

The paradox *can* be resolved (Tolhurst et al., 2002) by remembering that we are concerned not with equal increments of response magnitude but with *equally discriminable increments* of response. Because low response magnitudes suffer less variability than high ones, more of the code steps can fall at low firing rates. Many cortical neurons might give non-uniform, kurtotic responses yet still contribute to a maximum entropy, histogram equalised code for natural contrasts.

Acknowledgements

The preliminary studies for this project were funded by the Image Interpretation Initiative of the SERC. JSL received a research studentship from DERA; MC received a studentship from the MRC. We are very grateful to D.L. Ringach, M.J. Hawken, and R.Shapley for allowing us to use their unpublished data and for performing the analyses on our behalf. We are grateful to Dr. B. Willmore for interesting and helpful discussions.

References

Albrecht, D. G., & Hamilton, D. B. (1982). Striate cortex of monkey and cat: contrast response function. *Journal of Neurophysiology, 48*, 217–237.

Anzai, A., Bearse, M. A., Freeman, R. D., & Cai, D. Q. (1995). Contrast coding by cells in the cat's striate cortex—monocular vs binocular detection. *Visual Neuroscience, 12*, 77–93.

Atick, J. J. (1992). Could information theory provide an ecological theory of sensory processing? *Network, Computation in Neural Systems, 3*, 213–251.

Atick, J. J., & Redlich, A. N. (1992). What does the retina know about natural scenes? *Neural Computation, 4*, 196–210.

Attwell, D., & Laughlin, S. B. (2001). An energy budget for signalling in the grey matter of the brain. *Journal of Cerebral Blood Flow and Metabolism, 21*, 1135–1145.

Baddeley, R. J., Abbott, L. F., Booth, M. C. A., Sengpiel, F., Freeman, T., Wakeman, E. A., & Rolls, E. T. (1997). Responses of neurons in primary and inferior temporal visual cortices to natural scenes. *Proceedings of the Royal Society B, 264*, 1775–1783.

Baddeley, R. J., & Hancock, P. J. (1991). A statistical analysis of natural images matches psychophysically derived orientation tuning curves. *Proceedings of the Royal Society B, 246*, 219–223.

Baker, G. E., Thompson, I. D., Krug, K., Smyth, D., & Tolhurst, D. J. (1998). Spatial frequency tuning and geniculocortical projections in the visual cortex (areas 17 and 18) of the pigmented ferret. *European Journal of Neuroscience, 10*, 2657–2668.

Balasubramanian, V., Kimber, D., & Berry, M. J. (2001). Metabolically efficient information processing. *Neural Computation, 13*, 799–815.

Barlow, H. B. (1989). Unsupervised learning. *Neural Computation, 1*, 295–311.

Bell, A. J., & Sejnowski, T. J. (1997). The 'Independent Components' of natural scenes are edge filters. *Vision Research, 37*, 3327–3338.

Blake, R., & Petrakis, I. (1984). Contrast discrimination in the cat. *Behavioural Brain Research, 12*, 155–162.

Bonds, A. B. (1989). Role of inhibition in the specification of orientation selectivity of cells in the cat striate cortex. *Visual Neuroscience, 2*, 41–55.

Boynton, G. M., Demb, J. B., Glover, G. H., & Heeger, D. J. (1999). Neuronal basis of contrast discrimination. *Vision Research, 39*, 257–269.

Bradley, A., & Ohzawa, I. (1986). A comparison of contrast detection and discrimination. *Vision Research, 26*, 991–997.

Brady, N., & Field, D. J. (2000). Local contrast in natural images: normalisation and coding efficiency. *Perception, 29*, 1041–1055.

Britten, K. H., Shadlen, M. N., Newsome, W. T., & Movshon, J. A. (1992). The analysis of visual motion—a comparison of neuronal and psychophysical performance. *Journal of Neuroscience, 12*, 4745–4765.

Burton, G. J., & Moorhead, I. R. (1987). Colour and spatial structure in natural scenes. *Applied Optics, 26*, 157–170.

Campbell, F. W., & Kulikowski, J. J. (1966). Orientation selectivity of the human visual system. *Journal of Physiology, 187*, 437–445.

Clatworthy, P. L., Chirimuuta, M., Lauritzen, J. S., & Tolhurst, D. J. (2001). Computer models of contrast coding by pools of neurons in primary visual cortex (V1). *Journal of Physiology, 536P*, 41–42.

Croner, L. J., Purpura, K., & Kaplan, E. (1993). Response variability in retinal ganglion-cells of primates. *Proceedings of the National Academy of Sciences, 90*, 8128–8130.

Dan, Y., Atick, J. J., & Reid, R. C. (1996). Efficient coding of natural scenes in the lateral geniculate nucleus: experimental test of a computational theory. *Journal of Neuroscience, 16*, 3351–3362.

Dean, A. F. (1981a). The relationship between response amplitude and contrast for cat striate cortical neurones. *Journal of Physiology, 318*, 413–427.

Dean, A. F. (1981b). The variability of discharge of simple cells in the cat striate cortex. *Experimental Brain Research, 44*, 437–440.

Dean, A. F., & Tolhurst, D. J. (1986). Factors influencing the temporal phase of response to bar and grating stimuli for simple cells in the cat visual cortex. *Experimental Brain Research, 62*, 143–151.

De Valois, R. L., Albrecht, D. G., & Thorell, L. G. (1982). Spatial frequency selectivity of cells in macaque visual cortex. *Vision Research, 22*, 545–559.

De Valois, R. L., Yund, E. W., & Heppler, N. (1982). The orientation and direction selectivity of cells in macaque visual cortex. *Vision Research, 22*, 531–544.

Field, D. J. (1987). Relations between the statistics of natural images and the response properties of cortical cells. *Journal of the Optical Society of America A, 4*, 2379–2394.

Field, D. J. (1994). What is the goal of sensory coding? *Neural Computation, 6*, 559–601.

Field, D. J., & Brady, N. (1997). Visual sensitivity, blur and the sources of variability in the amplitude spectra of natural scenes. *Vision Research, 37*, 3367–3383.

Field, D. J., & Tolhurst, D. J. (1986). The structure and symmetry of simple-cell receptive-field profiles in the cat's visual cortex. *Proceedings of the Royal Society B, 228*, 379–400.

Foley, J. M. (1994). Human luminance pattern-vision mechanisms: masking experiments require a new model. *Journal of the Optical Society of America A, 11*, 1710–1719.

Gardner, J. L., Anzai, A., Ohzawa, I., & Freeman, R. D. (1999). Linear and nonlinear contributions to orientation tuning of simple cells in the cat's striate cortex. *Visual Neuroscience, 16*, 1115–1121.

Geisler, W. S., & Albrecht, D. G. (1995). Bayesian-analysis of identification performance in monkey visual-cortex—nonlinear mechanisms and stimulus certainty. *Vision Research, 35*, 2723–2730.

Geisler, W. S., & Albrecht, D. G. (1997). Visual cortex neurons in monkeys and cats: detection, discrimination and identification. *Visual Neuroscience, 14*, 897–919.

Geisler, W. S., Perry, J. S., Super, B. J., & Gallogly, D. P. (2001). Edge co-occurrence in natural images predicts contour grouping performance. *Vision Research, 41*, 711–724.

Gilbert, C. D. (1977). Laminar differences in receptive field properties of cells in cat primary visual cortex. *Journal of Physiology, 268*, 391–421.

Gottschalk, A. (2002). Derivation of the visual contrast response function by maximizing information rate. *Neural Computation, 14*, 527–542.

van Hateren, J. H. (1992). A theory of maximizing sensory information. *Biological Cybernetic, 68*, 23–29.

van Hateren, J. H., & van der Schaaf, A. (1998). Independent component filters of natural images compared with simple cells in primary visual cortex. *Proceedings of the Royal Society B, 265*, 359–366.

Heeger, D. J. (1992a). Normalization of cell responses in cat striate cortex. *Visual Neuroscience, 9*, 181–197.

Heeger, D. J. (1992b). Half-squaring in responses of cat simple cells. *Visual Neuroscience, 9*, 427–443.

Heeger, D. J., Huk, A., Geisler, W. S., & Albrecht, D. G. (2000). Spikes versus BOLD: what does neuroimaging tell us about neuronal activity? *Nature Neuroscience, 3*, 631–633.

Hyvarinen, A., & Hoyer, P. O. (2001). A two-layer sparse coding model learns simple and complex receptive fields and topography from natural images. *Vision Research, 41*, 2413–2423.

Ikeda, H., & Wright, M. J. (1975). Spatial and temporal properties of "sustained" and "transient" neurones in area 17 of the cat's visual cortex. *Experimental Brain Research, 22*, 363–383.

Itti, L., Koch, C., & Braun, J. (2000). Revisiting spatial vision: toward a unifying model. *Journal of the Optical Society of America A, 17*, 1899–1917.

Jones, J. P., & Palmer, L. A. (1987). An evaluation of the two-dimensional Gabor filter model of simple receptive fields in the cat striate cortex. *Journal of Neurophysiology, 58*, 1233–1258.

Kiper, D. C., & Kiorpes, L. (1994). Suprathreshold contrast sensitivity in experimentally strabismic monkeys. *Vision Research, 34*, 1575–1583.

Knill, D. C., Field, D. J., & Kersten, D. (1990). Human discrimination of fractal images. *Journal of the Optical Society of America A, 7*, 1113–1123.

Kontsevich, L. L., Chen, C. C., & Tyler, C. W. (2002). Separating the effects of response nonlinearity and internal noise psychophysically. *Vision Research, 42*, 1771–1784.

Kremers, J., Silveira, L. C. L., & Kilavik, B. E. (2001). Influence of contrast on the responses of marmoset lateral geniculate cells to drifting gratings. *Journal of Neurophysiology, 85*, 235–246.

Laughlin, S. B. (1981). A simple coding procedure enhances a neuron's information capacity. *Zeitschrift fur Naturforschung Section C Biosciences, 36*, 910–912.

Laughlin, S. B. (1983). Matching coding to scenes to enhance efficiency. In O. J. Braddick, & A. C. Sleigh (Eds.), *Physical and Biological Processing of Images* (pp. 42–52). Berlin: Springer-Verlag.

Lauritzen, J. S., & Tolhurst, D. J. (2000). A model of simple-cell contrast processing and normalisation in the mammalian visual cortex. *Journal of Physiology, 526P*, 158–159.

Law, C. C., & Cooper, L. N. (1994). Formation of receptive fields in realistic visual environments according to the Bienenstock, Cooper, and Munro (BCM) theory. *Proceedings of the National Academy of Sciences USA, 91*, 7797–7801.

Legge, G. E., & Foley, J. M. (1980). Contrast masking in human vision. *Journal of the Optical Society of America, 70*, 1458–1471.

Levy, W. B., & Baxter, R. A. (1996). Energy efficient neural codes. *Neural Computation, 8*, 531–543.

Logothetis, N. K., Pauls, J., Augath, M., Trinath, T., & Oeltermann, A. (2001). Neurophysiological investigation of the basis of the fMRI signal. *Nature, 412*, 150–157.

Lythgoe, J. N. (1991). Evolution of visual behaviour. In J. R. Cronly-Dillon, & R. L. Gregory (Eds.), *Vision and visual dysfunction: vol. II. Evolution of the eye and visual system* (pp. 3–14). London: Macmillan.

Marcelja, S. (1980). Mathematical description of the responses of simple cortical cells. *Journal of the Optical Society of America, 70*, 1297–1300.

Marr, D. (1970). A theory for cerebral neocortex. *Proceedings of the Royal Society B, 176*, 161–234.

Marr, D. (1982). *Vision*. San Francisco: W.H. Freeman & Co.

Movshon, J. A., Thompson, I. D., & Tolhurst, D. J. (1978). Spatial and temporal contrast sensitivity of neurones in areas 17 and 18 of the cat's visual cortex. *Journal of Physiology, 283*, 101–120.

Nachmias, J., & Sansbury, R. V. (1974). Grating contrast: discrimination may be better than detection. *Vision Research, 14*, 1039–1042.

Naka, K. I., & Rushton, W. A. H. (1966). S-potentials from colour untis in the retina of fish (*Cyprinidae*). *Journal of Physiology, 185*, 536–555.

Olshausen, B. A., & Field, D. J. (1997). Sparse coding with an overcomplete basis set: a strategy employed by V1? *Vision Research, 37*, 3311–3325.

Osorio, D., & Vorobyev, M. (1996). Colour vision as an adaptation to frugivory in primates. *Proceedings of the Royal Society B, 263*, 593–599.

Parraga, C. A., Troscianko, T., & Tolhurst, D. J. (2000). The human visual system is optimised for processing the spatial information in natural visual images. *Current Biology, 10*, 35–38.

Peli, E. (1990). Contrast in complex images. *Journal of the Optical Society of America A, 7*, 1113–1123.

Regan, B. C., Julliot, C., Simmen, B., Vienot, F., Charles Dominique, P., & Mollon, J. D. (2001). Fruits, foliage and the evolution of primate colour vision. *Philosophical Transactions of the Royal Society B, 356*, 229–283.

Reich, D. S., Mechler, F., & Victor, J. D. (2001). Temporal coding of contrast in primary visual cortex: when, what and why. *Journal of Neurophysiology, 85*, 1039–1050.

Ringach, D. L., Hawken, M. J., & Shapley, R. (1997). Dynamics of orientation tuning in macaque primary visual cortex. *Nature, 387*, 281–284.

Ruderman, D. L. (1994). The statistics of natural images. *Network, Computation in Neural Systems, 5*, 517–548.

Sclar, G., Maunsell, J. H. R., & Lennie, P. (1990). Coding of image-contrast in central visual pathways of the macaque monkey. *Vision Research, 30*, 1–10.

Scwartz, O., & Simoncelli, E. P. (2001). Natural signal statistics and sensory gain control. *Nature Neuroscience, 4*, 819–825.

Sengpiel, F., Baddeley, R. J., Freeman, T. C. B., Harrad, R., & Blakemore, C. (1998). Different mechanisms underlie three inhibitory phenomena in cat area 17. *Vision Research, 38*, 2067–2080.

Smyth, D., Willmore, B., Thompson, I. D., Baker, G. E., & Tolhurst, D. J. (in press). The receptive-field organisation of simple cells in primary visual cortex (V1) of ferrets under natural scene stimulation. *Journal of Neuroscience*.

Srinivasan, M. V., Laughlin, S. B., & Dubs, A. (1982). Predictive coding: a fresh view of inhibition in the retina. *Proceedings of the Royal Society B, 216*, 427–459.

Tadmor, Y., & Tolhurst, D. J. (1994). Discrimination of changes in the secondorder statistics of natural and synthetic images. *Vision Research, 34*, 541–554.

Tadmor, Y., & Tolhurst, D. J. (2000). Calculating the contrasts that retinal ganglion cells and LGN neurones encounter in natural scenes. *Vision Research, 40*, 3145–3157.

Thomson, M. G. A., & Foster, D. H. (1997). Role of second- and third-order statistics in the discriminability of natural images. *Journal of the Optical Society of America A, 14*, 2081–2090.

Tolhurst, D. J. (1989). The amount of information transmitted about contrast by neurones in the cat's visual cortex. *Visual Neuroscience, 2*, 409–413.

Tolhurst, D. J. (1996). The limited contrast-response of single neurones in cat striate cortex and the distribution of contrast in natural scenes. *Journal of Physiology, 497*, 64.

Tolhurst, D. J., & Barfield, L. P. (1978). Interactions between spatial frequency channels. *Vision Research, 18*, 951–958.

Tolhurst, D. J., & Dean, A. F. (1990). The effects of contrast on the linearity of spatial summation of simple cells in the cat's striate cortex. *Experimental Brain Research, 79*, 288–582.

Tolhurst, D. J., & Dean, A. F. (1991). Evaluation of a linear model of directional selectivity in simple cells of the cat's striate cortex. *Visual Neuroscience, 6*, 421–428.

Tolhurst, D. J., & Heeger, D. J. (1997). Comparison of contrast-normalization and threshold models of the responses of simple cells in cat striate cortex. *Visual Neuroscience, 14*, 293–309.

Tolhurst, D. J., Movshon, J. A., & Dean, A. F. (1983). The statistical reliability of single neurons in cat and monkey visual cortex. *Vision Research, 23*, 775–785.

Tolhurst, D. J., Movshon, J. A., & Thompson, I. D. (1981). The dependence of response amplitude and variance of cat visual cortical neurones on stimulus contrast. *Experimental Brain Research, 41*, 414–419.

Tolhurst, D. J., & Tadmor, Y. (2000). Discrimination of spectrally-blended natural images: optimisation of the human visual system for encoding natural images. *Perception, 29*, 1087–1100.

Tolhurst, D. J., Tadmor, Y., & Chao, T. (1992). The amplitude spectra of natural images. *Ophthalmic and Physiological Optics, 12*, 229–232.

Tolhurst, D. J., & Thompson, I. D. (1981). On the variety of spatial frequency selectivities shown by neurons in area 17 of the cat. *Proceedings of the Royal Society B, 213*, 183–199.

Tolhurst, D. J., Smyth, D., Thompson, I. D., Willmore, B., Chirimuuta, M., & Clatworthy, P. L. (2002). Experimental and computational study of the sparse responses of simple cells in striate cortex (V1): implications for models of the sparse-coding of information in natural scenes. *FENS Abstracts, 1*, 083.18.

Vinje, W. E., & Gallant, J. L. (2000). Sparse coding and decorrelation in primary visual cortex during natural vision. *Science, 287*, 1273–1276.

Vogels, R., Spileers, W., & Orban, G. A. (1989). The response variability of striate cortical neurons in behaving monkey. *Experimental Brain Research, 77*, 432–436.

Walker, G. A., Ohzawa, I., & Freeman, R. D. (1999). Asymmetric suppression outside the classical receptive field of the visual cortex. *Journal of Neuroscience, 19*, 10536–10553.

Wiener, M. C., Oram, M. W., Liu, Z., & Richmond, B. J. (2001). Consistency of encoding in monkey visual cortex. *Journal of Neuroscience, 15*, 8210–8221.

Willmore, B., & Tolhurst, D. J. (2001). Characterising the sparseness of neural codes. *Network, Computation in Neural Systems, 12*, 255–270.